Journal of Statistical Physics, Vol. 90, Nos. 1/2, 1998

A New Method for Analysis of the Fluid Interaction with a Deformable Membrane

Cyrus K. Aidun[1,3] and Dewei W. Qi[1,2]

Received February 27, 1996; final July 17, 1997

The lattice Boltzmann cellular automaton method has been successfully extended for analysis of fluid interactions with a deformable membrane or web. The hydrodynamic forces on the solid web are obtained through computation of the fluid flow stress at the moving boundary using the lattice Boltzmann method. Analysis of solid boundary deformation or vibration due to hydrodynamic force is based on Newtonian dynamics and a molecular dynamic type approach.

KEY WORDS: Fluid dynamics; deformable membrane; wed vibration; hydrodynamic forces; Newtonian dynamics.

1. INTRODUCTION

There is a large class of industrial processes which involve transport of deformable belts, tapes and sheets across open spans. Operations ranging from paper making machines to printing and coating processes are a few examples. Interaction between the moving web or membrane and surrounding fluids may cause the web to vibrate. The vibration, or flutter, in the open spans may cause problems such as cracks, buckling and web breaks.

Fundamental knowledge and understanding of the dynamic instability of webs in fluids are important in these industrial processes. The motion of

[1] Institute of Paper Science and Technology, and School of Mechanical Engineering at Georgia Institute of Technology, Atlanta, Georgia 30318.

[2] Current address: Department of Paper and Printing Science and Engineering, Western Michigan University, Kalamazoo, Michigan 49008.

[3] To whom correspondence should be addressed.

0022-4715/98/0100-0145$15.00/0

a web or sheet in fluid depends on the hydrodynamic forces at the solid-fluid interface as described by the thread-line model,[1]

$$m\frac{\partial^2 w}{\partial t^2}+2mV\frac{\partial^2 w}{\partial x\,\partial t}+(mV^2-T)\frac{\partial^2 w}{\partial x^2}+D\frac{\partial^4 w}{\partial x^4}=F(x,t) \tag{1}$$

where m is mass per unit area of the web, w is the displacement in the thickness direction, t is time, V is the velocity of the moving web in horizontal direction, T is the tension of the web, D is the bending stiffness, and the term $F(x, t)$ represents the hydrodynamic stress exerted on the top and bottom surfaces of the web. The second term in Eq. 1 is the Coriolis force and the third term is the centrifugal and restoring force. We consider a simple case in which a finite web with length L is placed in a continuum fluid and V is zero (corresponding to experiments on a stationary web placed inside a wind tunnel), thus Eq. 1 reduces to

$$m\frac{\partial^2 w}{\partial t^2}-T\frac{\partial^2 w}{\partial x^2}+D\frac{\partial^4 w}{\partial x^4}+=F(x,t) \tag{2}$$

In order to analyze the effects of tension on web flutter, as a first step we neglect the stiffness term (which is small for flexible webs). In other words, $|T(\partial^2 w/\partial x^2)| \gg |D(\partial^4 w/\partial x^4)|$, as described by Chang,[3] thus the equation reduces to the well-known wave equation,

$$m\frac{\partial^2 w}{\partial t^2}-T\frac{\partial^2 w}{\partial x^2}=F(x,t) \tag{3}$$

To solve this problem, we have to obtain hydrodynamic force, $F(x, t)$, which couples Eq. 3 with the Navier–Stokes equations. In this work, the lattice Boltzmann simulations have been employed to obtain the hydrodynamic forces, $F(x, t)$, through mass and momentum conservation equations of the fluid flow at the moving interface between the solid web and the fluid. To solve Eq. 3, the web is discretized into segments and the Newtonian dynamic simulations are applied to each segment. Nondimensional terms are used throughout this paper. The computational principle and procedures for the fluid phase and the fluid-solid interaction rules in the lattice Boltzmann equation are outlined in the next section along with a numerical example for verification of the lattice Boltzmann method. The method of web discretization and the Newtonian dynamics for solving the web deformation are described in Section 3. The numerical results of web deformation and vibration are presented in Section 4. Some conclusions are drawn in the final section.

2. LATTICE BOLTZMANN SIMULATION AND MOVING BOUNDARY CONDITIONS

The lattice Boltzmann cellular automaton method is a relatively new method that can be applied to the fluid flow problem.[4–9] Through a Chapman–Enskog like expansion,[10] it can be shown that the original Navier–Stokes equation can be recovered from the lattice Boltzmann equation. The numerical method can be effectively implemented on parallel processor computers because of its local nature.

In this work, a two-dimensional square lattice with unit spacing is used in the simulation.[10] Each node is connected by eight links to its nearest neighbors. Particles reside on nodes and move to their nearest neighbors along the links in unit time step. A portion of the fluid mass resides in the form of rest particles at each node. The velocity vectors $\mathbf{e}_{1i}$, $\mathbf{e}_{2i}$ $(i = 1,..., 4)$ are defined as

$$\mathbf{e}_{1i} = \left(\cos\frac{i-1}{2}\pi, \sin\frac{i-1}{2}\pi\right) \tag{4}$$

$$\mathbf{e}_{2i} = \sqrt{2}\left(\cos\left(\frac{i-1}{2}\pi + \frac{\pi}{4}\right), \sin\left(\frac{i-1}{2}\pi + \frac{\pi}{4}\right)\right) \tag{5}$$

along the perpendicular and diagonal directions. The lattice Boltzmann equation with single relaxation time is given by

$$f_{\sigma i}(\mathbf{x} + \mathbf{e}_{\sigma i}, t+1) - f_{\sigma i}(\mathbf{x}, t) = -\frac{1}{\tau}[f_{\sigma i}(\mathbf{x}, t) - f_{\sigma i}^{(0)}(\mathbf{x}, t)] \tag{6}$$

where $f_{\sigma i}$ is the single-particle distribution function, $f_{\sigma i}^{(0)}(\mathbf{x}, t)$ is the equilibrium distribution at $(\mathbf{x}, t)$ and τ is the single relaxation time. In our simulations, $f^{(0)}(\mathbf{x}, t)$ is taken as

$$f_{\sigma i}^{(0)}(\mathbf{x}, t) = A_\sigma + B_\sigma(\mathbf{e}_{\sigma i} \cdot \mathbf{u}) + C_\sigma(\mathbf{e}_{\sigma i} \cdot \mathbf{u})^2 + D_\sigma u^2 \tag{7}$$

with

$$\begin{aligned} &A_1 = \tfrac{1}{9}\rho, \quad B_1 = \tfrac{1}{3}\rho, \quad C_1 = \tfrac{1}{2}\rho, \quad D_1 = -\tfrac{1}{6}\rho \\ &A_2 = \tfrac{1}{36}\rho, \quad B_2 = \tfrac{1}{12}\rho, \quad C_2 = \tfrac{1}{8}\rho, \quad D_2 = -\tfrac{1}{24}\rho \\ &A_0 = \tfrac{4}{9}\rho, \qquad\qquad\qquad\quad D_0 = -\tfrac{2}{3}\rho \end{aligned} \tag{8}$$

where ρ is the mass density of fluid at the node. For this model, the kinematics viscosity is $\nu = (2\tau - 1)/6$, and the Reynolds number is defined as $Re = UN/\nu$ where U and N are the characteristic velocity and the

lattice size. With this equilibrium distribution, the Navier–Stokes equations can be derived using the Chapman–Enskog expansion.[10]

To guarantee accuracy of results, the boundary conditions at the interface between solid and fluid particles have to be correctly imposed. If the solid is stationary, a no-slip boundary condition is easily implemented by using bounce-back method. For moving solid, Ladd[4, 5] recognizes that the bounceback method has to be modified to match the velocity of the solid surface at the boundary node and to account for the momentum transfer to the solid particle. The nodes on either side of the boundary surface are treated in an identical fashion, so that fluid fills the whole volume of space. By allowing exchanging of population density between boundary nodes adjacent to the surface, Ladd's collision rule is given by

$$f_{\sigma i'}(\mathbf{x}, t+1) = f_{\sigma i}(\mathbf{x}, t_+) - 2B_\sigma(\mathbf{e}_{\sigma i} \cdot \mathbf{u}_b) \tag{9}$$

Here $\mathbf{x}$ is the position of the node adjacent to the solid surface which is moving with velocity $\mathbf{u}_b$, i' denotes the reflected direction and i, the incident direction, points opposite to i'. Equation (9) correctly accounts for the exchange of momentum, however, it results in transfer of fluid across the solid surface. The extra mass is equal to the second term on the RHS of (9). Recently, Aidun and Lu[11] and Aidun *et al.*[12] have presented a different boundary rule for impermeable solid surfaces to prevent fluid particles from penetrating into the solid phase. In most cases where inertia is not important, the presence of fluid inside the particle has no adverse effect and the results will be accurate, as shown by Ladd[5] and Aidun, *et al.*[12] (Fig. 4 in ref. 12). In some cases where particle inertial becomes important. In the case when fluid is allowed to enter the solid particle, the mass of the particle used in the Newton's equation for particle motion should be adjusted to account for the mass of the fluid inside the particle. As long as the fluid inside the particle moves as a solid body, the results will be accurate with this adjustment. Otherwise the viscosity of the fluid inside the particle has to be adjusted according to force the fluid inside the particle to behave as a solid body, as explained by Ladd.[5] No adjustments are required with the impermeable solid particles method, as outlined by Aidun *et al.* In this work, the web is treated as a zero thickness membrane with both sides exposed to the fluid. Therefore, there is no interior fluid or artificial inertia.

The velocity vector $\mathbf{u}_b$ depends not only on the translational and the angular velocity of the solid, but also on the position where the fluid particles collide with the solid, and the colliding directions, that is

$$\mathbf{u}_b = \mathbf{U} + \boldsymbol{\Omega} \times (\mathbf{x} + \tfrac{1}{2}\mathbf{e}_{\sigma i} - \mathbf{X}) \tag{10}$$

where $\mathbf{U}$ is the translational velocity of the suspension, $\mathbf{\Omega}$ the angular velocity with respect to the center of mass, and $\mathbf{X}$ is the position vector of the center.

For a given link (σi) at a node, the force on the solid is given by

$$\mathbf{F}_{\sigma i} = \begin{cases} 2(f_{\sigma i}(\mathbf{x}, t_+) - B_\sigma \mathbf{u}_b \cdot \mathbf{e}_{\sigma i})\, \mathbf{e}_{\sigma i}, & \text{incident links} \\ 0 & \text{otherwise} \end{cases} \tag{11}$$

whereas the torque, $\mathbf{K}_{\sigma i}$ with respect to the center of mass, $\mathbf{X}$, is given by

$$\mathbf{K}_{\sigma i} = (\mathbf{x} + \tfrac{1}{2}\mathbf{e}_{\sigma i} - \mathbf{X}) \times \mathbf{F}_{\sigma i} \tag{12}$$

Cylinder Couette flow is selected to numerically verify the correctness of the above collision rules. Unlike planar Couette flow, the fluid density at the node adjacent to the solid surface is not locally conserved in the cylinder Couette flow. The population at the fluid node adjacent to the solid surface will exchange with that at the solid node adjacent to the surface in a manner where total population density at the fluid and solid nodes is conserved. However, the combined momentum of solid and fluid is conserved. In the test considered, the radius R_1 of the inside cylinder is 40.56 lattice units, the radius R_2 of the outside cylinder is 100.54, the inside cylinder is fixed, the velocity v_2 of the outside cylinder is 0.1, the density ρ is 2.7, and the kinematic viscosity ν is 0.1667. The velocity profile along the radial direction using the lattice-Boltzmann method is compared with the analytical solution,[13] given by

$$v = \frac{(R_2 v_2 - R_1 v_1)}{R_2^2 - R_1^2} R + \frac{R_1 v_1 R_2^2 - R_1^2 R_2 v_2}{R_2^2 - R_1^2} \frac{1}{R} \tag{13}$$

The result is in excellent agreement with the analytical solution, as shown in Fig. 1. The value 11.09 of the torque K exerted on the inside cylinder in the numerical solution is also compared with analytical value of 11.05 obtained from the following formula,[13]

$$K = 4\pi\rho\nu \frac{R_1^2 R_2 v_2 - R_2^2 R_1 v_1}{R_2^2 - R_1^2}$$

The error for the torque is less than 0.4%. This indicates that the hydrodynamic force generated by the shear stress at the wall is accurately captured by the numerical method employed in this study.

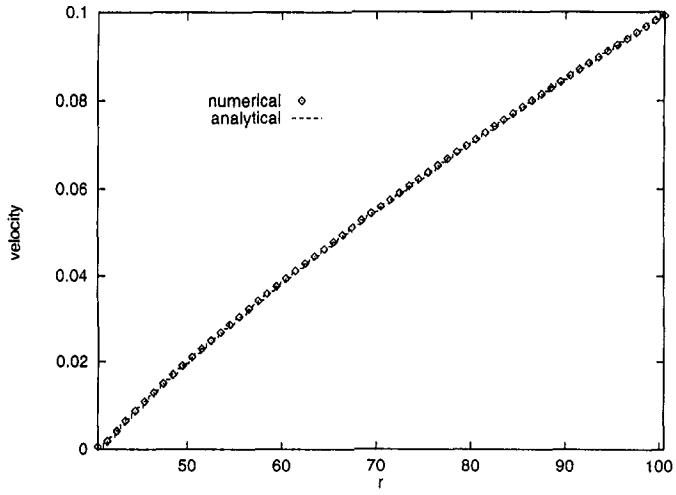

Fig. 1. Comparison of velocity distribution of numerical simulation with that of analytical solution in cylinder Couette flows.

3. DISCRETIZED SHEET AND NEWTONIAN ALGORITHM

We turn to solve the wave Eq. 3 and compute the web deformation. Motivated by the lattice Boltzmann method for fluid phase (i.e., discretizing time and space), we also discretized the solid web or sheet as shown in Fig. 2. The web is divided into equal segments with length Δx. The tensions T are exerted on the ends of the segment in the tangle direction. Assuming that the displacement w is very small and only happens in the y-direction, i.e. the hydrodynamic force in the x-direction is neglected), we balance the hydrodynamic forces and tension on the segment in the y-direction and obtain the following Newtonian equations,

$$F\,\Delta x + T\tan\alpha_2 + T\tan\alpha_1 = \Delta x m a \tag{14}$$

$$F + T\frac{1}{\Delta x}\left(\left.\frac{\Delta w}{\Delta x}\right|_2 - \left.\frac{\Delta w}{\Delta x}\right|_1\right) = ma \tag{15}$$

$$F + T\frac{\partial^2 w}{\partial x^2} = m\frac{\partial^2 w}{\partial t^2} \tag{16}$$

where $a(t)$ is the acceleration of the center of mass of the segment and T is the tension exerted at the end of each segment. In the limit as Δx approaches zero, the original wave equation governing the deformation of

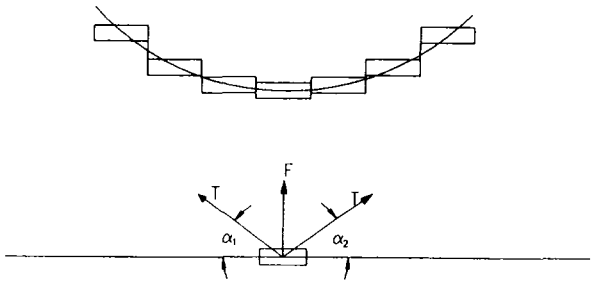

Fig. 2. The top of the figure shows that the web is discretized. The bottom of the figure shows that the tensions T in α_1 and α_2 directions and the hydrodynamic force F are exerted on one segment web.

the web is recovered. Therefore, formula 14 becomes the main equation to solve the motion of each segment.

In Eq. 14, $\tan\alpha_1$ and $\tan\alpha_2$ are simply obtained from slopes of the line connecting the centers of mass of the adjacent segments. It is assumed that each segment of the web is laid along the x-direction, and the length of the web segment is chosen to fit, one lattice unit, as shown in Fig. 3. The hydrodynamic force F on the segment can be calculated by summing over all $\mathbf{F}_{\sigma i}$ in Eq. 11 exerted on the segment. The node at the ends of each segment may be shared by two adjacent segments. Consequently, the shared-node velocity is taken to be the average of the two neighbor segments, and the hydrodynamic force at the shared-node is then divided equally between the two segments. In order to obtain the correct value of the force on each segment, our algorithms should be able to recognize 9 different topological patterns constructed by a mid-segment, its right and left neighbor segments to track the movement of the web during vibration. Some of the patterns are given in Fig. 3. The boundary nodes adjacent to the web segment from

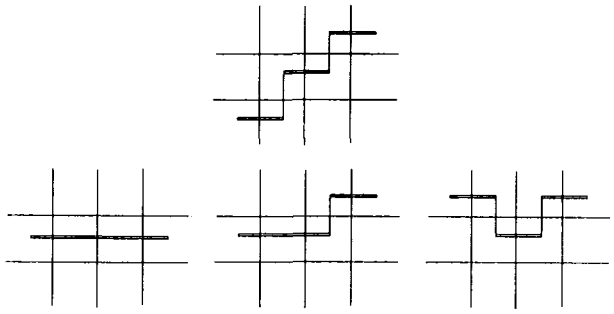

Fig. 3. The parallel bars are the segments of the web. Four patterns are shown.

the bottom are assigned number 1, and those from top are assigned number 2 to track the configuration of the web. Whenever one of mass centers of segments moves across a lattice, configuration of the web is updated to calculate the hydrodynamic forces correctly for each the segment.

In order to solve Eq. 14, the Newtonian algorithm can be employed to update the position and velocity of each segment of the web. There are many schemes available in the field of molecular dynamic simulations.[14, 15] The general idea of Newtonian simulation is as follows. Given the molecular (each segment of the web in this work) positions $\mathbf{r}$, velocities $\mathbf{v}$ and other dynamic information at time t, we attempt to obtain the positions, velocities, etc. at a later time $t+\delta t$, to a sufficient degree of accuracy. The equations are solved on a step-by-step basis in time. The choice of the time interval δt will depend somewhat on the method of solution, but δt should be small enough to guarantee convergence and accuracy. A more in-depth discussion of the effect of time step on the dynamic behavior of differential equation systems is presented by Poliashenko and Aidun.[16] In this study, we use a so-called half-step "leap-frog" scheme,[15] presented by

$$\mathbf{v}(t+\tfrac{1}{2}\delta t) = \mathbf{v}(t-\tfrac{1}{2}\delta t) + \delta t\mathbf{a}(t) \tag{17}$$

$$\mathbf{r}(t+\delta t) = \mathbf{r}(t) + \delta t\,\mathbf{v}(t+\tfrac{1}{2}\delta t) \tag{18}$$

The stored quantities are the current position $\mathbf{r}(t)$ and acceleration $\mathbf{a}(t)$ together with the mid-step velocities $\mathbf{v}(t-\frac{1}{2}t)$. The velocity Eq. 17 is implemented first, and the velocities leap over the coordinates to give the next mid-step values $\mathbf{v}(t+\frac{1}{2}\delta t)$. During this step, the current velocities may be calculated from

$$\mathbf{v}(t) = 0.5[\mathbf{v}(t+\tfrac{1}{2}\delta t) + \mathbf{v}(t-\tfrac{1}{2}\delta t)] \tag{19}$$

Following this, Eq. 18 is used to propel the position once more ahead of the velocities. We can easily prove that the error in Eq. 18 is $O(\delta t^4)$. In this work, Newtonian dynamic time step δt is set to 0.01 lattice unit. The acceleration $\mathbf{a}(t)$ at each Newtonian time step can be calculated from hydrodynamic forces and tension.

To examine the accuracy of our numerical method for the wave equation using a combination of discretized web with Newtonian dynamic simulation, we perform a numerical test. In the verification test, the total length, L, of the web is 150, $m=137$, hydrodynamic force is set to zero, and tension is 0.6. Initial velocity of the web is zero, and initial displacement is given by

$$w = A \sin\frac{\pi x}{L}$$

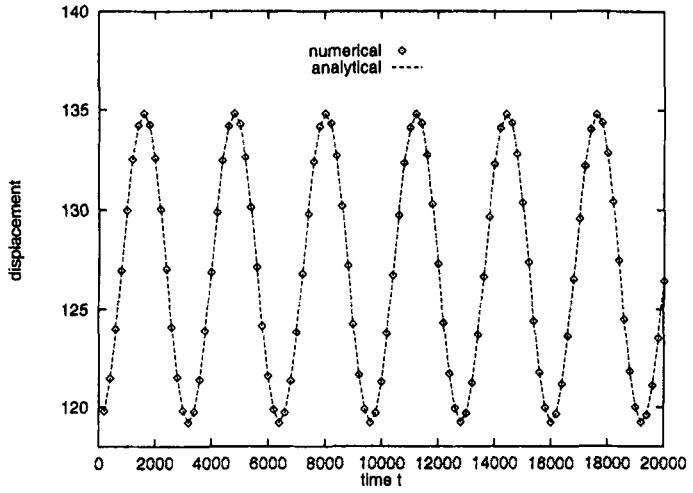

Fig. 4. Comparison of displacement at center point of web varying with time in the numerical testing with that in an analytical solution.

where amplitude A is equal to -7.8. The two ends of the web are fixed and displacement is allowed only in the y-direction. A total of 20,000 lattice time steps (2,000,000 Newtonian time steps) are considered. The numerical result is compared with the analytical solution and plotted in Figs. 4 for displacement. The It has been shown that the Newtonian dynamic approach with our web discretization scheme is quit accurate and reliable.

4. NUMERICAL SIMULATION FOR SHEET FLUTTER

Now we will conduct several numerical simulations by combining the methods discussed in Section 2 and 3 to investigate the interaction between fluid and a deformable web.

A straight web with length $L = 156$ is initially placed along the x-direction in the center of a simulation box of 256 by 256 in node. The initial velocity is given by

$$\frac{dw}{dt} = A \sin \frac{\pi x}{L}$$

where A is -0.02 and x in the above equation starts at the left end of the web. The fluid density is 2.7, and the kinematic viscosity v is 0.008. The fluid is driven by injecting fluid particles into the left side of the simulation box with an average velocity of 0.1. Reynolds number for the flow is

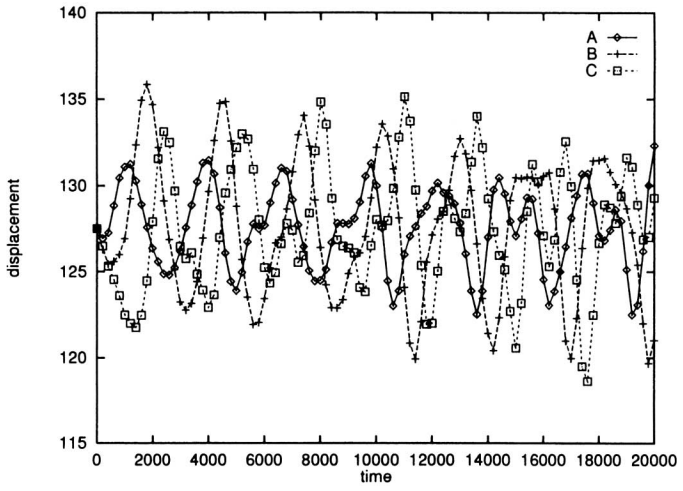

Fig. 5. The displacements at points A, B, and C of the web (see text) vary with time for the case of tension $T = 0.48$.

about 3,200. A no-slip boundary condition is imposed on the top and bottom side walls of the box. After the system reaches equilibrium, the web is allowed to deform and oscillate. Hydrodynamic forces on each segment depend on the configuration of the deformable web according to the mechanism presented in Section 3. Whenever one of the segments moves

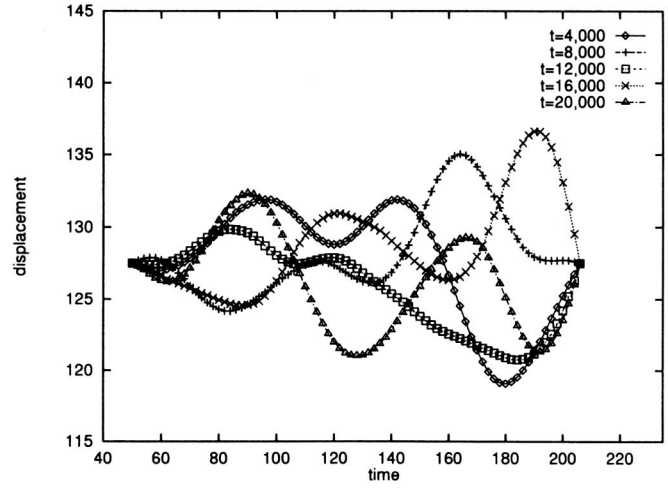

Fig. 6. The web configurations at every 4,000 lattice time step interval for the case of tension $T = 0.48$.

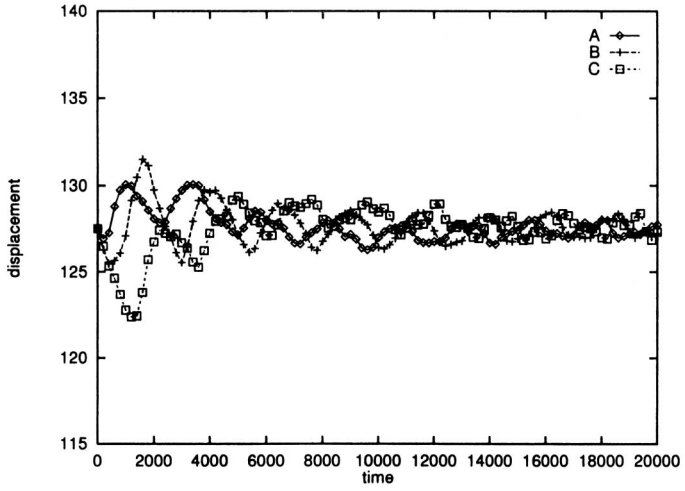

Fig. 7. The displacements at points A, B, and C of the web vary with time for the case of tension $T = 0.7$.

across a lattice, the hydrodynamic force on each segment is updated. To cancel staggered momentum, the hydrodynamic forces are updated in the average of every two lattice time steps. In order to guarantee the accuracy in solving Eq. 14, Newtonian dynamic time step is taken as 0.01 lattice time unit, i.e., one lattice time step is divided into 100; thus the velocity and

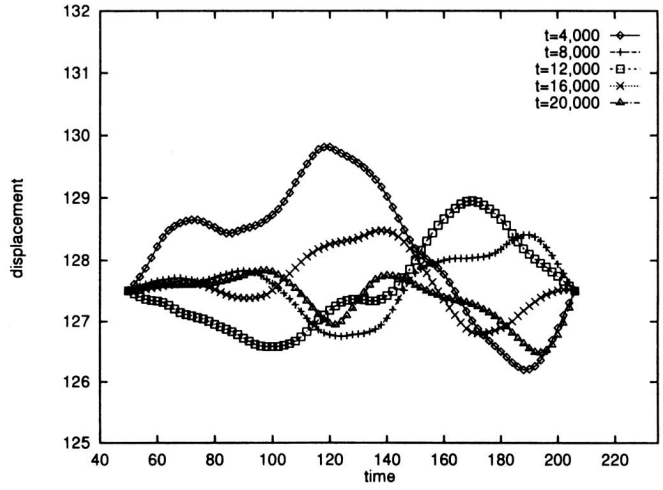

Fig. 8. The web configurations at every 4000 lattice time step interval for the case of tension $T = 0.7$.

position of each segment are updated at every Newtonian time step to take account of variation of $\tan \alpha_1$ and $\tan \alpha_2$ in Eq. 14 during vibration, while keeping averaged hydrodynamic force unchanged within 2 lattice time steps (200 Newtonian time steps). Each computational experiment for web fluterring runs 20,000 lattice time steps (2,000,000 Newtonian time steps).

Figure 5 shows the displacements at point A, 1/4 of length of the web, point B, 1/2 of the web, and point C, 3/4 of the web, varying with time for minimum tension $T = 0.48$. It is observed that flutter occurs and remains without damping. To investigate the effects of tension on the fluttering of web, the tension T is varied from 0.48 to 0.9. Figure 6 shows the displacements at every 4,000 lattice time step interval for the same case.

The fluid flows from the left of the simulation box to the right and generates larger displacement in the right side, as shown in these two figures. Also, it is observed that high mode vibrations are rapidly developed, even though the initial velocity is in the lowest mode. This is evidence of the strong interaction between the fluid and the web. When tension increases from 0.48 to 0.7, the vibrations are gradually damped and the amplitude decreases, as shown in Fig. 7 for the displacement at points A, B and C of the web, and in Fig. 8 for web configuration at every 4000 lattice time step interval. Figures 9 and 10 show the dynamics of the web at $T = 0.9$. The figures clearly show that at this tension the oscillation is completely suppressed and the web can be only buckled. These results are consistent with wind tunnel experiments of Chang[3] and Chang and

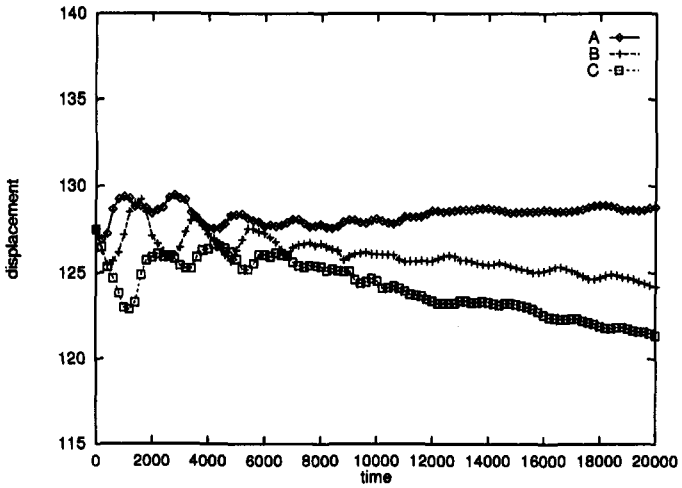

Fig. 9. The displacements at points A, B, and C of the web vary with time for the case of tension $T = 0.9$.

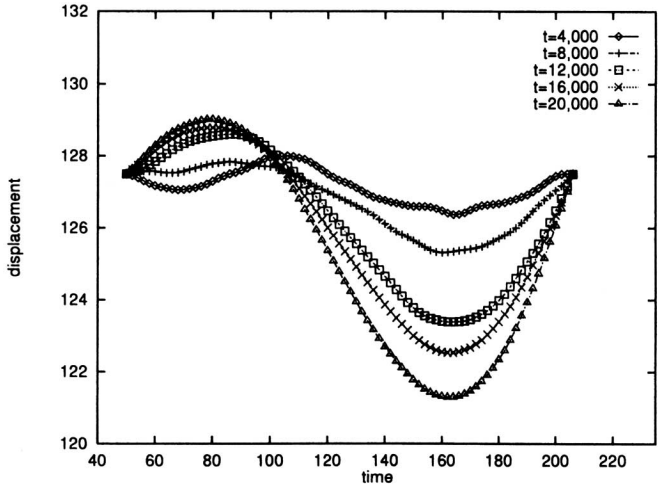

Fig. 10. The web configurations at every 4,000 lattice time step interval for the case of tension $T = 0.9$.

Moretti.[2] In practice, it is usually observed that the edge of the web which is under lower tension could flutter while the mid-section of the web remains stationary.

5. CONCLUSION

We have extended the lattice Boltzmann cellular automation method to analyze the dynamics of fluid interactions with deformable solid boundaries. The fluid flow and solid deformable equations are fully coupled in the discrete time-space domain. The key is to project the solid boundary onto the discrete domain and to analyze the solid deformation based on the hydrodynamic forces obtained from the lattice Boltzmann simulations and appropriate Newtonian dynamic simulations. Because of the local nature of the operation in the method, solving of the equation on the massive parallel processors results in a very efficient numerical method for simulation of fluid flow problems with deformable boundaries.

ACKNOWLEDGMENTS

This study has been supported by the National Science Foundation through grant CTS-9258667, and by industrial matching contributions. The computations are conducted, in part, by using Cray T3D in the Pittsburgh Supercomputing Center which is funded by the National Science Foundation.

REFERENCES

1. Y. B. Chang, P. M. Moretti, *Tappi* March, 231, (1991).
2. Y. B. Chang, P. M. Moretti, *Sheet Flutter & Windage Problems Seminar. Tappi notes*, 14 (1991). *Web Handling*, ASME 67 (1992).
3. Y. B. Chang, "An Experimental and Analytical Study of Web Flutter," Ph.D. Dissertation, School of Mechanical and Aerospace Engineering, Oklahoma State University, Stillwater (1990).
4. A. J. C. Ladd, *J. Fluid Mech.*, "Numerical simulations of particulate suspensions via a discretized Boltzmann equation, Part I," **271**:285 (1994).
5. A. J. C. Ladd, *J. Fluid Mech.*, "Numerical simulations of particulate suspensions via a discretized Boltzmann equation, Part II," **271**:311 (1994).
6. U. Frisch, B. Hasslacher, and Y. Poemeau, *Phys. Rev. Lett.*, "Lattice-Gas Automaton for the Navier-Stokes Equation," **56**:1505 (1986).
7. S. Wolfram, *J. Stat. Phys.*, "Cellular Automaton Fluids 1: Basic Theory," **45**:471 (1986).
8. G. McNamara, and G. Zanetti, *Phys. Rev. Lett.*, "Use of the Boltzmann Equation to Simulate Lattice-Gas Automaton," **61**:2332 (1988).
9. P. Bhatnagar, E. P. Gross, and M. K. Krook, *Phys. Rev.*, "A Model for Collision Processes in Gas: I. Small amplitude Processes in Charged and Neutral One-Component Systems," **94**:511 (1954).
10. Shuling Hou, Qisu Zou, Shixi Chen, Gary D. Doolen and A. Cogley, "Simulation of Incompressible Navier–Stokes Fluid Flows Using a Lattice Boltzmann Method" *J. Computational Physics* **118**:329 (1993).
11. C. K. Aidun and Y. Lu, "Lattice Boltzmann Simulation of Solid Suspensions with Impermeable Boundaries" *J. Statistical Physics* **81**: (no. 1/2), 49, (1995).
12. C. K. Aidun, Y. Lu, and E.-J. Ding, "Dynamic Simulation of Particules Suspended in Fluid," *Proc. of the 6th International Symp. on Solid-Liquid Flows, FEDSM/ASME*, Vancouver, Canada, June 22, 1997.
13. H. L. Dryden, F. P. Murnaghan, and H. Bateman, *Hydro-dynamics* (1956).
14. D. H. Heermann, *Computer Simulation Methods in Theoretical Physics*, Springer-Verlag Berlin Heidelberg New York (1986).
15. R. W. Hockney, *Methods Comput. Phys.* **9**:136 (1970), P. Potter, *Computational Physics*, Wiley, New York, Verlet, *L. Phys. Rev.* **165**:201 (1968), **159**:98 (1967).
16. M. Poliashenko and C. K. Aidun, "Computational Dynamics of Ordinary Differential Equations," *International J. Bifurcation and Chaos* **5**:1 (1995).